Martin Dadić
martin.dadic@fer.hr

University of Zagreb
Faculty of Electrical Engineering and Computing
Unska 3, 10 000 Zagreb, Croatia

Tomislav Župan
tzupan@koncar-institut.hr

KONČAR - Electrical Engineering Institute, Inc,
Transformer Department, R&D Section,
Fallerovo šetalište 22, 10000 Zagreb, Croatia

Teaching Magneto-Thermal Coupling Using Thomson's Levitating Ring Experiment

SUMMARY

The levitating ring experiment is presented as a method for teaching magneto-thermal interactions. The complete electromagnetic model of a problem is given, together with the insight in thermal analysis. The factors for determining the vertical displacements are explained, and an elegant method for indirect measurement of induced current in the ring is introduced. The whole apparatus is explained in detail so an accurate computer model can be made. Several simulation approaches are given, and all prove the applicability in teaching coupled problems using laboratory experiments and computer modeling.

KEYWORDS

magnetic levitation, electromagnetic forces, electrodynamics

NTRODUCTION

Thomson's levitating ring is a standard demonstration in teaching undergraduate physics, which explains Faraday's and Lenz laws, as well as the forces on the current-carrying conductor in magnetic field. It was shown initially in 1887 by Elihu Thomson as a launching ring experiment, and in 1890 John A. Fleming demonstrated a levitating variant, which is widely used in teaching electrodynamic theory [1],[2]. Due to a nonlinear character of the device, it is also used in teaching control systems, either using nonlinear models [3]-[5] or linear ones [6]-[11]. There are also papers describing the control systems for magnetic suspension [2],[12]-[15], which is another approach to the levitation experiments. In control-systems environment, the device is often modeled using the black-box approach, or only the parameters needed for the control systems synthesis (like excitation coil inductance) are calculated using the electromagnetic theory. In general physics, the underlying electromagnetic phenomena are often oversimplified [16].

At all universities, courses in undergraduate electromagnetic theory usually have some kind of a laboratory. With the wide spreading of numerical analysis software, it is tempting to include them in the student's laboratory. At many universities the whole laboratory is based only on the finite element (FEM) simulation, and at some other the laboratory is based solely on the experiments.

The main purpose of this paper is to describe a successful application of the levitating ring experiment in such a laboratory, where the experiments are linked with the coupled electromagnetic and thermal FEM simulation. A real experiment helps the students to better understand the purpose, limits and the application areas of numerical analysis software, and to better visualize object and phenomena that they are modeling.

In addition, all the elements of the experiments are carefully analyzed and thoroughly explained from the engineer's point of view, and an elegant way to indirectly measure the current in the ring is described.

In application, some of the measurements or calculations may be omitted and the guidelines for such modifications are given in the paper. With all presented elements, the experiment can be also applied in a laboratory of undergraduate electromechanics.

The paper is organized as follows: in Section II the analytical electromagnetic model is given. Section III presents the laboratory model and Section IV explains the factors contributing to the elevation of the ring. The thermal analysis is given in Section V. Section VI introduces the method for indirectly measuring the induced current in the ring. Finally, results of measurements and computer simulations are given in Sections VII and VIII, respectively.

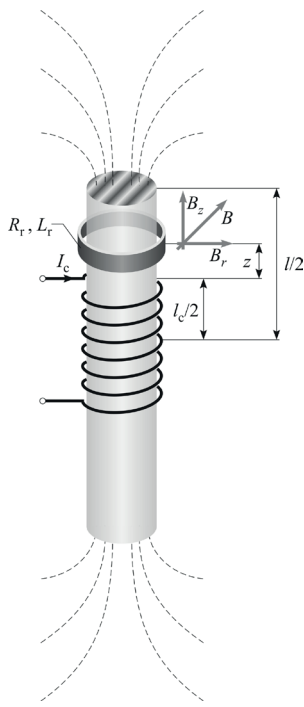# ANALYTICAL ELECTROMAGNETIC MODEL

Fig. 1. Working principle of the levitating ring apparatus

The apparatus consists of a copper coil circularly wound around the laminated ferromagnetic core. The core protrudes upwards out of the coil to guide the ring. The ring, made out of non-magnetic conducting material (copper or aluminum) is stacked on the core and initially lies reclined to the coil. If we connect the coil to a proper sinusoidal voltage source, the ring starts to levitate at the height determined by the amount of current flowing through the coil.

The working principle of the described device is explained in [10], [17] and shown in Fig. 1. Current flowing through the coil will create the magnetic field. Magnetic field lines inside the core will roughly be parallel with the core axis. Outside the core, they will form closed curved lines. Therefore, in each position of the ring, the coil's magnetic field will have both axial B_z and radial B_r components, which we can express in cylindrical coordinate system as

$$\vec{B}_z = B_{z0} \sin(\omega t)\vec{a}_z, \tag{1}$$

$$\vec{B}_r = B_{r0} \sin(\omega t)\vec{a}_r. \tag{2}$$

Here, B_{z0} and B_{r0} represent the peak axial and radial magnetic flux densities, ω represents the angular frequency $\omega = 2\pi f$, where f is the frequency of the sinusoidal source, t represents time and $\vec{a}_z$ and $\vec{a}_r$ stand for axial and radial unit vectors, respectively.

The induced electric field around the perimeter of the ring is related with the axial component of the magnetic flux density B_z. Assuming that the magnetic flux density throughout the surface of the ring's cross section is uniform and that the ring thickness is negligible, we obtain the induced electric field using the Faraday's law of electromagnetic induction:

$$\nabla \times \vec{E} = -\frac{\partial B}{\partial t}, \tag{3}$$

$$\vec{E}(b,t) = -\frac{\omega b B_{z0}}{2} \cos(\omega t)\vec{a}_\alpha, \tag{4}$$

where b is the radius of the ring. Now we can calculate the induced voltage in the ring, using

$$e = \oint_l \vec{E} \cdot d\vec{l} = -\omega \pi b^2 B_{z0} \cos(\omega t). \tag{5}$$

If the impedance of the ring is $Z_r = \sqrt{R_r^2 + (\omega L_r)^2}$, where R_r and L_r represent ring's resistance and inductance, respectively, the induced current in the ring will be

$$i_r = \frac{e}{Z_r} = -\frac{\omega \pi b^2 B_{z0}}{Z_r} \cos(\omega t - \varphi_r) = I_{r0} \cos(\omega t - \varphi_r). \tag{6}$$

Here, φ_r is the ring's impedance phase angle:

$$\varphi_r = \arctan \frac{\omega L_r}{R_r}. \tag{7}$$

If the ring is placed in a magnetic field with magnetic flux density $\vec{B}$, the force acting on an infinitesimal segment dl of the ring is

$$d\vec{F} = i_r d\vec{l} \times \vec{B}. \tag{8}$$

Therefore, the total force on the ring is equal to

$$F = i_r 2\pi b B_{r0} \sin(\omega t). \tag{9}$$

As can be seen, only the radial component of the magnetic flux density affects the axial force which causes the levitation of the ring. The field's axial component causes the radial force on the ring and integrating it over the ring's perimeter the result is zero (if the ring is placed horizontally). Obviously, this manifests as the radial stress on the ring, trying to compress it inwards, towards its axis. As can be seen in (9), the force is time-varying. Therefore, its average value is significant when calculating the axial displacement of the ring:

$$F_{avg} = 2\pi b I_{r0} B_{r0} \frac{1}{2\pi / \omega} \int_0^{2\pi/\omega} \cos(\omega t - \varphi_r)\sin(\omega t)\, dt = \tag{10}$$

$$= \pi b I_{r0} B_{r0} \sin \varphi_r.$$

If m is the mass of the ring, g the gravitational acceleration, c the viscous damping coefficient and x the elevation of the ring, the motion equation can be written as

$$m\frac{d^2 x}{dt^2} + c\frac{dx}{dt} = F(x) - m g. \tag{11}$$

The gravitational pull opposes the electromagnetic force and, after the initial transient movement, the ring levitates at the point where these two forces cancel each other.

In reality, the magnetic flux density and its radial and axial components cannot be calculated analytically. The same holds for the inductance, and the problem is even more complicated with the thermal dependence of the ring's resistance. Increasing the current in the ring, it dissipates more power which causes it to warm up and thus its resistance increases. Consequently, the increased resistance lowers the current and the force, causing the ring to gradually "sink" until a stable working point is reached. The whole process of heat dissipation is also calculable only using numerical methods, and since two processes (magnetic and thermal) are coupled it is tempting to apply coupled numerical analysis. In addition, with the finite dimensions of the ring, the lumped-parameter calculation becomes inaccurate both for electromagnetic and thermal calculation.

LABORATORY MODEL

The coil is made out of 576 turns of copper wire (0.95 mm in diameter) circularly wound in a hollow cylinder form with 18.6 and 31.8 mm inner and outer diameter, respectively. The core is made out of laminated non-oriented electrical steel, assembled out of 30 sheets. Because of the easier assembling, it's cross section is rectangular (9.85 mm x 10.1 mm) with overall height equal to 200 mm. Paper ruler is attached to one side of the core for measuring the height of the levitating ring. The detailed layout of the model, together with the dimensions, is visible in Fig. 2.
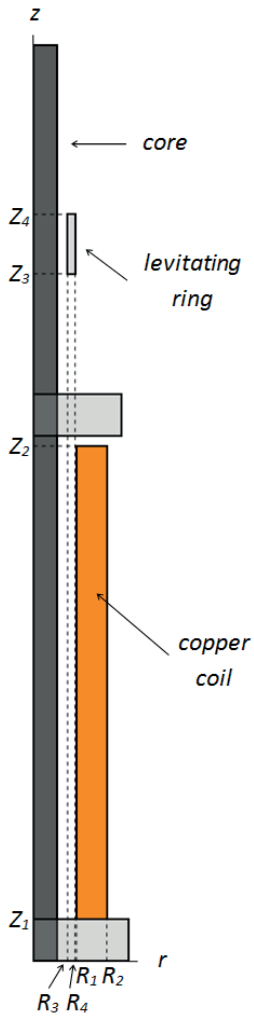
Fig. 2. Side view of the apparatus. Coil parameters are R_1=9.3 mm, R_2=15.9 mm, Z_1=9.15 mm, Z_2=112.45 mm. Ring parameters are R_3=7.375 mm, R_4=9 mm, Z_4-Z_3=13 mm. Core parameters are (W x D x H) 10.1 x 9.85 x 200 mm

TABLE I
ALUMINUM ALLOY 5005-O PHYSICAL, ELECTRICAL AND THERMAL PROPERTIES [17]

Property	Value
density	2.70 g/cm^3
electrical resistivity	3.32 x 10^{-8} Ωm
temperature coefficient	0.0036 K^{-1}
specific heat capacity	0.900 J/g°C
thermal conductivity	200 W/mK

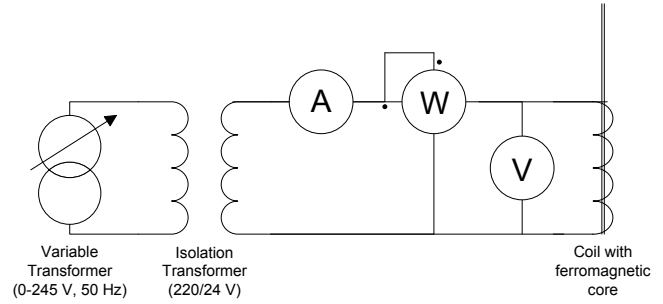Fig. 3. Levitating ring apparatus.

Fig. 4. Connection diagram of the levitating ring apparatus.

The ring is made out of aluminum alloy 5005-O, whose physical, electrical and thermal properties are given in Table I [18]. It is 13 mm high with the inner and the outer radius equal to 7.375 mm and 9 mm, respectively. For the sinusoidal voltage-regulating source, Iskra MA 4803 variable transformer was used (245 V, 50 Hz). It is connected to the isolation transformer (220/24 V) in order to ensure the safety of non-professionals (e.g. students) using the levitating ring apparatus. Two true RMS digital multimeters (UNI-T UT60E) are used for measuring the voltage of the coil and the current flowing through it. For measuring the electric power of the coil, Iskra OES0101 digital wattmeter is used (accuracy class of 0.1 at the 40-60 frequency range). Finally, FLIR i7 thermal camera is used in order to accurately measure the temperature of the ring. Since the emissivity of the polished aluminum is 0.04-0.06 [19], a standard black electrical tape was cut in a square 4 mm wide and attached to the ring. The emissivity of such a tape is 0.96 and therefore the temperature of the ring can be precisely measured using the thermal camera. Whole apparatus demonstrating the levitating ring experiment is visible in Fig. 3 and the connection diagram in Fig 4.

HEIGHT OF THE RING AND ITS VERTICAL DISPLACEMENT

In [17] the influence of the phase angle of the ring's impedance on the vertical displacement is presented. Nevertheless, the influence of the ring's height on the phase angle is only briefly elaborated. In [10] the inductance of the ring is calculated for a circular ring. In this section, an engineering perspective will be given to the calculation of the inductance of the applied ring, which was in the form of a hollow cylinder.

The alternating current flowing through the coil induces the electromagnetic force which pulls the ring upwards. Equation (10) shows that three main parameters dictate the value of the force: the induced current flowing through the ring I_{r0}, the radial component of the magnetic flux density B_{r0} and the ratio of the ring's inductance over its resistance $\sin \varphi_r$ (see (7)). These three parameters and their influence on the elevation of the levitating ring are explained next.

The electromagnetic force will decrease with the elevation, since the magnetic flux density decreases with distance from the coil [20]. The ring will levitate at the point where that force is equal to the gravitational pull on the ring.

In order to calculate the factor $\sin \varphi_r$, the inductance and the resistance of the ring have to be obtained. Since the ring used in the experiment has the shape of a hollow cylinder, the resistance can be calculated using the thin-wall solenoid approximation

$$R_r = \rho \frac{l}{A}. \tag{12}$$

Here, ρ is the electrical resistance of the material of the ring, l is the mean circumference of the ring and A is the area of the cross section of the ring. We obtain

$$R_r = \frac{\rho \pi}{h} \cdot \frac{b_o + b_i}{b_o - b_i}, \tag{13}$$

where h is the height of the ring and b_o and b_i represent the outer and the inner radius of the ring, as visible in Fig. 5.

The calculation of the inductance of the circular ring with rectangular cross section is not trivial. Since the ring in this experiment is relatively thin, the same thin-wall solenoid approximation can be used. Self inductance can then be obtained using [21]

$$L_r = \frac{4\mu_0 b_{mean}^2}{3h\beta k^3} \left(\left(2k^2 - 1\right)E\left(k\right) + \left(1-k^2\right)K\left(k\right) - k^3 \right). \quad (14)$$

Here, μ_0 is the permeability of air, b_{mean} is the ring's mean radius ($b_{mean} = \dfrac{b_o + b_i}{2}$) and $E\left(k\right)$ and $K\left(k\right)$ are the complete elliptic integrals of the first and the second kind. Factors β and k are calculated as follows:

$$\beta = \frac{h}{2b_{mean}}, \quad (15)$$
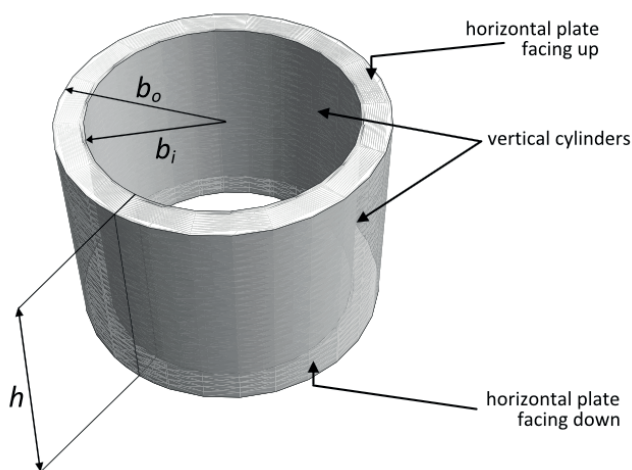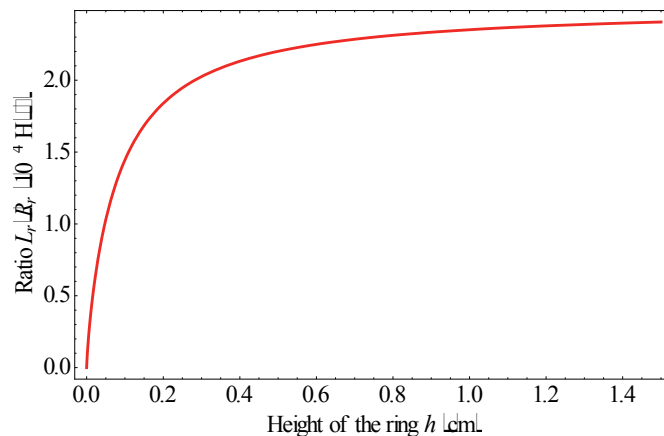
$$k = \sqrt{\frac{1}{1+\beta}}. \quad (16)$$

Fig. 6. Correlation of the ratio of the ring's inductance over its resistance with regards to the height of the ring. The geometry of the ring and its electrical resistivity is given in Fig. 2 and Table I.

Fig. 5. Aluminum ring in the form of a hollow cylinder.

TABLE III
PROPERTIES OF AIR [22]
(AT ATMOSPHERIC PRESSURE OF 101.3 kPA AND TEMPERATURE OF 300 K)

Symbol	Property	Value
g	gravitational acceleration	9.80665 m/s^2
β	thermal expansion coefficient (for air $\beta=1/T_\infty$)	0.0033 K^{-1}
v	kinematic viscosity	15.68 x 10^{-6} m^2/s
α	thermal diffusivity	22.16 x 10^{-6} m^2/s
k	thermal conductivity	0.02624 W/m K
ρ	density	1.177 kg/m^3
c_p	specific heat capacity	1005.7 J/kg K
Pr	Prandtl number	0.708

TABLE II
STEADY-STATE ELEVATION OF DIFFERENT RINGS
(I_{COIL}=1.5 A, INNER AND OUTER RADIUS ARE THE SAME FOR ALL THREE RINGS)

Ring's height (mm)	Elevation (mm)
3.1	4
6.3	29
13	52

Fig. 6 shows the correlation of the ratio of the ring's inductance over its resistance with regards to the height of the ring. It is clearly visible that the ratio increases, i.e. the character of the ring's impedance is increasingly inductive. Consequently, the parameter $\sin\varphi_r$ in (10) increases which means that the ring with greater height can achieve higher vertical displacement from the coil (its levitating point is higher). Using the laboratory model from Section III, the steady-state elevation of three rings with different heights is presented in Table II.

The induced current flowing through the ring I_{r0}, according to (6), is determined by the source frequency, axial component of the magnetic flux density, ring's radius and the impedance of the ring. Since the resistance of the ring is very low, the induced current tends to be relatively high. If the ring is kept levitating for a relatively long period of time, the ring's temperature will noticeably increase. Consequently, increasing the ring's temperature, its resistance increases as well, according to the linear approximation of temperature dependence

$$R_{r\vartheta} = R_r \left(1 + \alpha\left(\vartheta - 20°\text{C}\right)\right), \quad (17)$$

where ϑ is the temperature in the Celsius temperature scale, α is the temperature coefficient of the material of the ring, R_r is the ring's resist-

ance at $20°$C and $R_{r\vartheta}$ is the ring's resistance at the temperature ϑ. The increased resistance of the ring will cause the current flowing through it to decrease and hence the overall electromagnetic force exerted on the ring will decrease. As a consequence, the ring will slowly "sink" (its elevation will gradually fall) as the ring's temperature increases.

As can be seen from the abovementioned, the behavior of the levitating ring cannot be easily predicted or calculated. This justifies the usage of the levitating ring experiment in teaching control systems as described in the Section I. The number of overlapping physical effects makes this experiment well suitable in teaching engineering electrodynamics and electromagnetically and thermally coupled-problem solving, as well.

THERMAL ANALYSIS

Previous chapter explained the influence of the increased temperature of the ring on its elevation height. If the alternating source in the experiment apparatus is turned on for a long period of time, the levitating ring will finally come to a steady state and its elevation height will not further decrease with time. At that point the heat generated in the ring due to the power loss (Joule heating) will become equal to the heat dissipated from the ring to its surroundings. The mechanisms explaining the heat exchange are complicated and involve solving the convective heat transfer and the thermal

radiation equations. However, by neglecting or approximating some thermal effects, the thermal model of the ring may be analytically explained.

If a hot object is radiating energy to its cooler surroundings, the radiation heat loss rate can be expressed as

$$\dot{q}_{rad} = \varepsilon\sigma\left(T_s^4 - T_\infty^4\right)A, \tag{18}$$

where ε is the emissivity of the object, σ is the Stefan-Boltzmann constant ($\sigma = 5.6703\cdot10^{-8}$ W/m^{2}K^4), T_s is the surface temperature of an hot object (absolute, thermodynamic temperature in K), T_∞ is the temperature of the surroundings (also in K) and A is the area of the object. Since the ring in this experiment is made out of highly polished aluminum whose emissivity is around 0.04 [22], the heat dissipation by radiation can be neglected.

The convective heat transfer caused by the movement of the heated air around the levitating ring can be approximated using the analytical expressions for natural convection on vertical cylinders and on horizontal plates. The Newton's law of cooling states that the rate of convection heat transfer $\dot{q}_{conv}$ is

$$\dot{q}_{conv} = \frac{dQ}{dt} = h \cdot A\left(T_s - T_\infty\right), \tag{19}$$

where Q is the thermal energy (in joules), h is the convection heat transfer coefficient (W/m^{2}K), A is the surface area of the heat being transferred (m^2), T_s is the temperature of the object's surface (in K) and T_∞ is the temperature of the environment (in K).

The heat transfer coefficient h is characterized by the geometry of the object, its physical properties and the positioning in the environment. The four surfaces of the cylindrical ring, due to its sharp edges, can be approximated with the horizontal plate facing up, the horizontal plate facing down and two vertical cylinders, as illustrated in Fig. 5. The coefficient h is defined as

$$h = \frac{Nu \cdot k}{L}, \tag{20}$$

where Nu is the Nusselt number, k is the thermal conductivity of the material and L is the characteristic length of the surface. In order to calculate the Nusselt number, the Rayleigh number has to be defined as well:

$$Ra_L = \frac{g\beta}{\nu\alpha}\left(T_s - T_\infty\right)L^3. \tag{21}$$

All the parameters are defined in Table III. If, for the sake of simplicity, the air flow is assumed to be laminar, the Nusselt number for a horizontal plate facing up is [23]

$$Nu = \frac{1.4}{\ln\left(1 + \dfrac{1.4}{0.835\,C_{lam}Ra_L^{0.25}}\right)}. \tag{22}$$

The coefficient C_{lam} is defined as

$$C_{lam} = \frac{0.671}{\left(1 + \left(\dfrac{0.492}{Pr}\right)^{9/16}\right)^{4/9}}, \tag{23}$$

where Pr is the Prandtl number (Table III). The characteristic length is equal to the ratio of the plate surface area to its perimeter, which in this case is equal to

$$L = \frac{area}{perimeter} = \frac{\left(b_o^2 - b_i^2\right)\pi}{2\pi\left(b_o + b_i\right)} = \frac{b_o - b_i}{2}. \tag{24}$$

The Nusselt number for a horizontal plate facing down is equal to [23]

$$Nu = \frac{2.5}{\ln\left(1 + \dfrac{2.5}{0.527\,Ra_L^{0.2}}\left(1 + \left(\dfrac{1.9}{Pr}\right)^{0.9}\right)^{2/9}\right)}. \tag{25}$$

The characteristic length is given in (24). Finally, the Nusselt number for a vertical cylinder is [23]

$$Nu = Nu_{vp}\frac{\xi}{\ln\left(1 + \xi\right)}, \tag{26}$$

where Nu_{vp} is the Nusselt number for a vertical flat plate (i.e. neglecting the curvature of the cylinder),

$$Nu_{vp} = \frac{2.0}{\ln\left(1 + \dfrac{2.0}{C_{lam}Ra_L^{0.25}}\right)}. \tag{27}$$

Here, C_{lam} is given in (23), and the characteristic length L is equal to the height of the plate (the height of the cylinder in this case). Factor ξ takes into account the influence of the curvature and is defined as

$$\xi = \frac{1.8}{Nu_{vp}}\frac{L}{D}, \tag{28}$$

where D is the diameter of the cylinder.

Knowing the temperatures of the environment and of the object, using (18)-(28) the total heat transfer of the cylindrically shaped object can be calculated. However, since the dimensions of the ring are relatively small, the analytical equations given yield inaccurate results. Therefore, numerical methods with a more detailed approach should be used when trying to accurately model the thermal characteristics of the ring. The above-mentioned parameters are explained in order to become acquainted with the thermal analysis nomenclature and to have a more insight when simulating this experiment using a computer. There is a plenty of available literature with a more detailed approach to heat transfer theory and computational thermal analysis [22-26].

INDIRECT MEASUREMENT OF THE CURRENT IN THE RING

None of the papers dealing with the levitating ring experiment [1]-[16] present the method for measuring or calculating the induced current in the ring. One of the approaches would be to make an accurate thermal model of the ring. Since all the heat generated inside the ring comes from the Joule losses, the current can be obtained knowing the heat transfer from the ring to its surroundings. This can only be accurately achieved using the computational thermal analysis, which is out of scope of many electrical engineers. This section presents an indirect way of measuring the Joule losses. Thus, the induced current in the ring can be calculated more precisely.

If we connect the apparatus according to the connection diagram in Fig. 4, the real power measured will consist of Joule losses in the coil, hysteresis and eddy current losses in the ferromagnetic core and the Joule losses in the aluminum ring. The ferromagnetic core is laminated which minimizes the core losses caused by the eddy currents. If the core is made out of the low-loss material, the hysteresis losses will be significantly smaller in comparison with the coil losses. Furthermore, because of the open-core type, these losses will be reduced even more since the magnetic flux density inside the ferromagnetic core is low.

Keeping the current in the coil equal throughout the measurements, if P_{w2} is the measured real power with the levitating ring inserted and the P_{w1} without it, we can determine the Joule losses in the aluminum ring as the difference in measurements

$$P_{w2} - P_{w1} = I_r^2 R_{r,\vartheta}, \tag{29}$$

where $I_r = I_{r0}/\sqrt{2}$ is the effective value of the induced current in the ring. Using (17) and knowing the geometric and electrical properties of the ring together with its temperature, the current flowing through the ring is

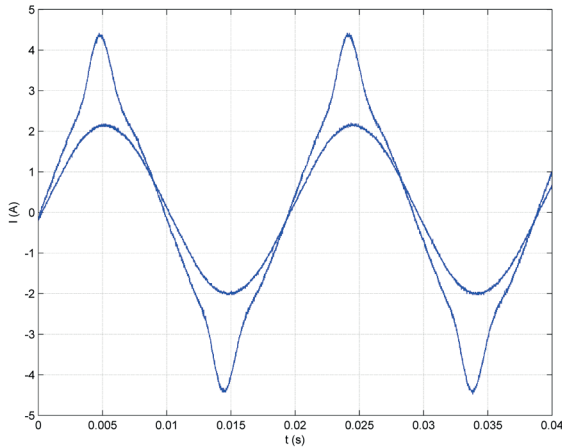$$I_r = \sqrt{\frac{P_{w2} - P_{w1}}{R_{r,\vartheta}}}. \tag{30}$$

Fig. 7. Measured waveforms of the excitation currents in the coil. At 1.5 A (RMS) the waveform is sinusoidal and at 2 A (RMS) the waveform is distorted due to the core's nonlinearity.

Excitation current in the coil has to be sinusoidal for the digital wattmeter used to be accurate. Therefore, we have to be in the linear part of the *B-H* curve of the ferromagnetic material of the core (i.e. the relative magnetic permeability of the material has to be constant). Fig. 7 shows the oscilloscope waveforms of the excitation currents at 1.5 A (RMS) which is practically sinusoidal, and at 2 A (RMS) where the nonlinearity of the core becomes apparent.

MEASUREMENTS

The measurements were done on apparatus explained in Section III. The excitation current in the coil was targeted at 1 A (RMS) and 1.5 A (RMS) and two sets of measurements were taken within a time frame of 10 minutes with the time step of 0.5 minute. Prior to the measurements and the insertion of the ring, the current through the coil was flowing long enough for the coil to reach a steady temperature. The elevation of the aluminum ring was measured at the upper side of the ring using the attached paper ruler, as visible in Fig. 3. The temperature readings were obtained using the thermal camera. The temperature of the surroundings was 28.6 °C and 29.0 °C and the real power of the coil without the ring inserted was P_{w1}=3.05 W and P_{w1}=1.45 W for the first and the second set, respectively.
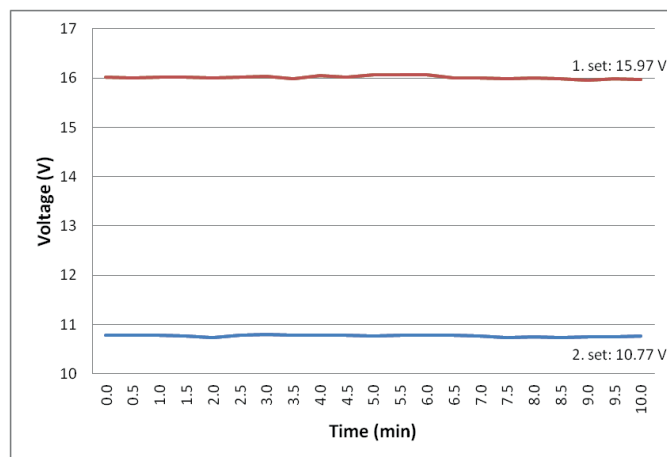

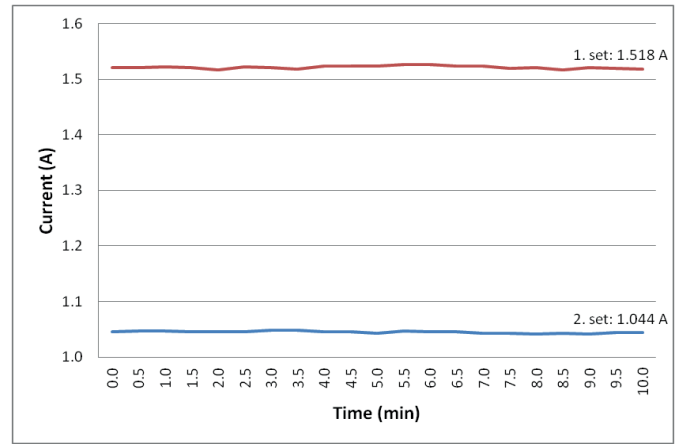Fig. 8. Voltage of the coil remained unchanged in time for both sets of measurements.

Fig. 9. Current inside the coil remained unchanged in time for both sets of measurements.
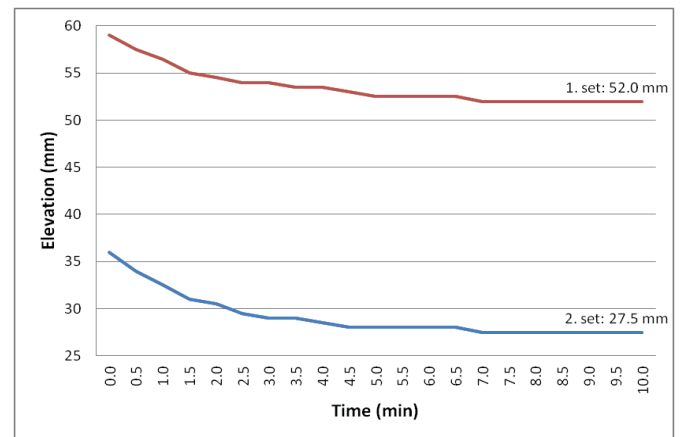

Fig. 10. Elevation of the ring gradually decreased in time until a steady state was achieved.
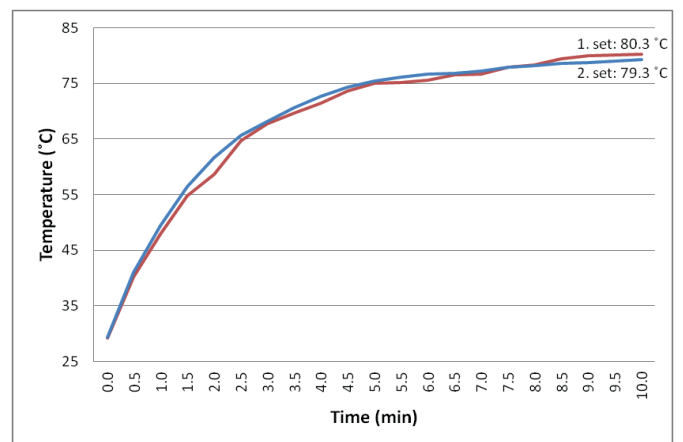

Fig. 11. Temperature of the ring increased in time.
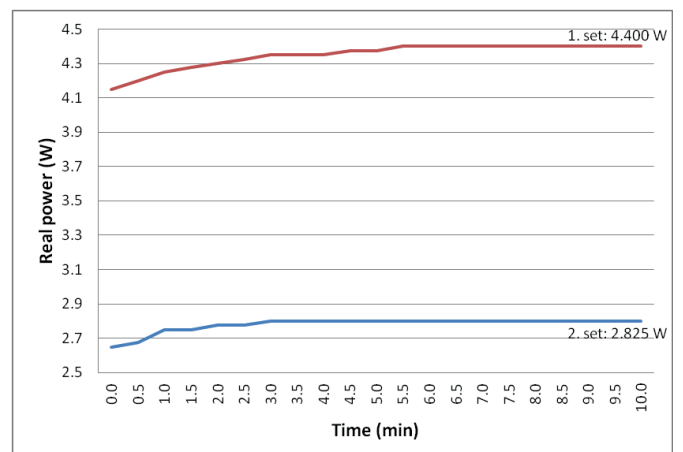

Fig. 12. Real power of the coil gradually increased in time until a steady state was achieved.
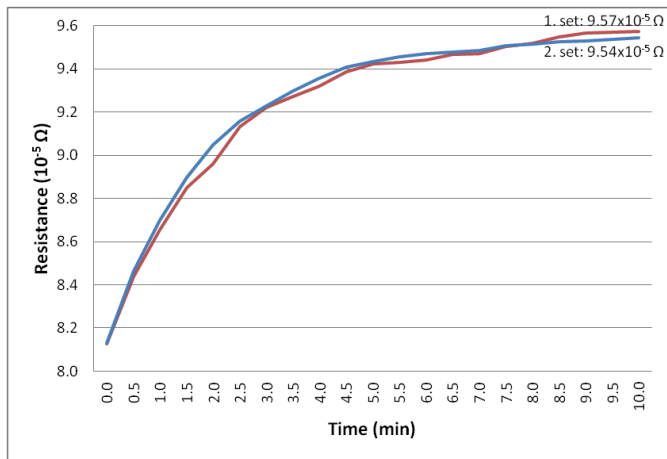
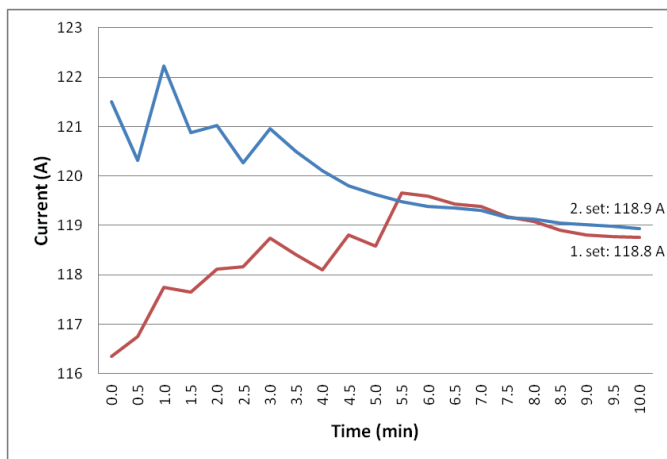Fig. 13. Calculated resistance of the ring as a function of time.

Fig. 14. Calculated current flowing through the ring as a function of time.

The voltage and the current of the coil remained unchanged throughout the measurements, as can be seen in Fig. 8-9. All the other measured parameters (elevation, temperature, real power) change until the steady state is achieved, as is visible in Fig. 10-12. Finally, Fig. 13 shows the calculated resistance of the ring using (17) and Fig. 14 the calculated current flowing through the ring using (30).

A number of conclusions can be deduced from the presented figures. If the voltage and the current of the coil remain unchanged (Fig. 8-9) and the overall real power gradually increases until a steady state is achieved (Fig. 12), obviously the power factor increases as well. This means that the phase angle between the voltage and the current decreases, i.e. the character of the impedance of the load becomes more and more resistive. The ring will levitate at the position where the magnetic force acting on it equals its own weight, as explained in Section II. Since the temperature of the ring rises (Fig. 11), its resistance rises as well (Fig. 13), meaning that the current flowing inside it should decrease. The magnetic force is now lower and it cannot compensate the pull of the ring's weight and the ring moves downwards. Now the ring is closer to the coil and the axial magnetic flux density increases which leads to the increased induced voltage in the ring (5). This increases the current in the ring and the magnetic force-weight equilibrium is achieved again. The calculated current flowing through the ring (Fig. 14) shows that, throughout the measurements, its value remains relatively constant.

COMPUTER SIMULATIONS

Described experiment of the levitating ring can be easily simulated on a computer using one of the available FEM electromagnetic/thermal software packages. The time needed to model it is relatively low which makes it ideal for a student computer-simulations project.

To completely model the levitating ring experiment, a transient analysis, which can deal with the gradual heating and "sinking" of the ring, should be made. However, the complexity of such an approach makes it appropriate only for senior-year student assignments. For an undergraduate level, another approach may be applicable. Doing the measurements first, final steady state values can be used as simulation parameters. Using Fig. 10, the ring can be placed at the proper elevation and applying the measured currents (Fig. 9) the magnetic force and current in the ring can be obtained. Also, if a coupled electromagnetic-thermal analysis is done, the final temperature of the ring can also be retrieved.

The simulations in this paper are done using the *Infolytica MagNet* and *ThermNet* software. Depending on the software licenses available at the certain universities, there are many approaches at computer modeling of the levitating ring experiment, as presented in the next subsections.

A.   3D Electromagnetic-Thermal Coupled Simulation

The levitating ring apparatus can be modeled using the geometric, electrical and physical properties from the Section III. A custom material is specified for the ring using the Table I. For the ferromagnetic core, an M270-35A non-oriented fully processed electrical steel is chosen based on the thickness and core losses [27]. Finally, a 98% IACS copper is used for modeling the coil. All the plastic protrusions and supports are omitted from the model since they do not affect its electromagnetic properties. Obviously, the teachers should choose the materials appropriate for their available equipment when setting up this project. For the thermal part of the simulation, only the ring is taken into consideration for the sake of simplicity. The four surfaces are modeled according to Section V and the temperature of the surroundings is set as in the measurements.

B,   2D Electromagnetic-Thermal Coupled Simulation

If only 2D modeling software is obtainable it can be used as well and still achieve satisfactory results. Since the ring and the coil can be modeled in 2D geometry, only the ferromagnetic core with rectangular cross section has to be approximated in 2D. A standard procedure of equaling the cross section areas can be used. If a rectangular cross section needs to be transformed into a circular one, the radius of a circular cross section has to be

$$R_{circular} = \sqrt{\frac{width \times depth}{\pi}}, \qquad (31)$$

which, in this case, using the data from Fig. 2, yields $R_{circular}$=5.62735 mm.

Obviously, the 2D approach can be used without the abovementioned approximation if a laboratory model is made with ferromagnetic cores with circular cross section.

C)   3D or 2D Electromagnetic Simulation

For a pure electromagnetic analysis, the thermal calculation can be omitted. The problem is then simpler, since no thermal modeling needs to be done. Using the measurements (Fig. 13), the final steady state temperature of the ring has to be defined in the simulation software used in order to accurately calculate the resistance and, therefore, the induced current flowing in the ring.

D)   Simulation Results

As with the measurements, the two sets of calculations were done. The results obtained using the different computer simulation approaches, together with the measured values, are presented in Tables IV-V.

The magnetic force in Tables IV-V is equaled to the calculated weight of the ring using the density from Table I and geometric parameters of the ring from Fig. 2. The total weight *G* of the ring calculated this way is

$$G = gm = g\gamma V = g\gamma h\pi \left(b_o^2 - b_i^2 \right), \quad (32)$$

where *g* is the gravitational acceleration, *m* is the mass of the ring, *V* is its volume and γ is the density of the ring (Table I).

As can be seen from the calculated results, the 3D electromagnetic-thermal coupled computer simulation provides, as expected, the results

TABLE IV
MEASURED AND CALCULATED RESULTS FOR THE LEVITATING RING
I_C = 1.518 A, *ELEVATION OF THE RING* = 52.0 MM, T$_{SURROUNDINGS}$ = 28.6 °C

Approach	Induced current (A)	Magnetic force (mN)	Temperature (°C)
Measurement	118.8	28.8[a]	80.3
3D Coupled	118.5	29.0	76.9
2D Coupled	111.6	24.9	71.5
3D Electromagnetic	117.4	28.5	80.3[b]
2D Electromagnetic	108.7	23.6	80.3[b]

[a] Gravitational pull calculated from the geometric parameters of the ring (Fig. 2) and its density (Table I) using (31)

[b] Temperature defined in the simulation

TABLE V
MEASURED AND CALCULATED RESULTS FOR THE LEVITATING RING
I_C = 1.044 A, *ELEVATION OF THE RING* = 27.5 MM, T$_{SURROUNDINGS}$ = 29.0 °C

Approach	Induced current (A)	Magnetic force (mN)	Temperature (°C)
Measurement	118.9	28.8[a]	79.3
3D Coupled	119.0	28.9	77.7
2D Coupled	113.0	24.7	72.9
3D Electromagnetic	118.5	28.6	79.3[b]
2D Electromagnetic	111.0	23.9	79.3[b]

[a] Gravitational pull calculated from the geometric parameters of the ring (Fig. 2) and its density (Table I) using (31)

[b] Temperature defined in the simulation

closest to the measured values. All the other simulation approaches offer results that are still quite satisfying and prove that, if full 3D licenses are not available, the levitating ring experiment can be modeled accurately.

CONCLUSIONS

Teaching electromagnetic theory can sometimes be a challenging task due to the complex mathematics used. The topic of levitation is appealing and interesting to students and can be an effective way in teaching engineering electrodynamics. A simple levitating ring experiment, which can be easily conducted at any electromagnetic laboratory, proves to be a practical demonstration of electromagnetic-thermal processes and a great example for teaching coupled-problem solving.

Computer simulations of the mentioned experiment can be done relatively effortlessly and can be used for student projects. Results obtained from simulations are in a good correlation with measurements and can explain the advantages of using computer modeling in designing electrical devices to students. A number of the simulation approaches, depending on the available software at the university, can be used and all produce satisfying results.

This paper presents a thorough analysis of the levitating ring experiment and its computer simulations and demonstrates it as an electromagnetic-thermal coupled problem adequate in teaching undergraduate electrodynamics and computer modeling.

REFERENCES

[1] R. J. Hill, »Teaching electro-dynamic levitation theory,« *IEEE Trans. Educ.*, vol. 33, no. 4, pp. 346-354, November 1990.

[2] M. T. Thompson, " Electrodynamic magnetic suspension—models, scaling laws, and experimental results," *IEEE Trans. Educ.*, vol. 43, no. 3, pp. 336-342, Aug. 2000.

[3] Z.-J. Yang, Y. Fukushima, S. Kanae, and K. Wada, "Robust non-linear output-feedback control of a magnetic levitation system by K-filter approach," *IET Control Theory Appl.*, vol. 3, iss. 7, pp. 852-864, 2009.

[4] S. A. Green and K. C. Craig, "Robust, digital, nonlinear control of magnetic-levitation systems," *J. Dyn. Sys., Meas., Control*, vol. 120, no. 4, pp. 488-495, Dec. 1998.

[5] S.-W. Park, "System development for education and design of a nonlinear controller with on-line algorithm," *Int. J. Control. Autom.*, vol. 1, no. 2, pp. 215-221, Jun. 2003.

[6] R. K. H. Galvão, T. Yoneyama, F. M. U. de Araújo, and R. G. Machado, "A simple technique for identifying a linearized model for a didactic magnetic levitation system," *IEEE Trans. Educ.*, vol. 46, no. 1, pp. 22-25, Feb. 2003.

[7] T. H. Wong, "Design of a magnetic levitation control system – an undergraduate project," *IEEE Trans. Educ.*, vol. E-29, no. 4, pp. 196-200, Nov. 1986.

[8] P. S. Shiakolas and D. Piyabongkarn, "Development of a real-time digital control system with a hardware-in-the-loop magnetic levitation device for reinforcement of controls education," *IEEE Trans. Educ.*, vol. 46, no. 1, pp. 79-87, Feb. 2003.

[9] R. Valle, F. Neves, R. de Andrade Jr., and R. M. Stephan, "Electromagnetic levitation of a disc," *IEEE Trans. Educ.*, vol. 55, no. 2, pp. 248-254, May 2012.

[10] N. Barry and R. Casey, "Elihu Thomson's jumping ring in a levitated closed-loop control experiment," *IEEE Trans. Educ.*, vol. 42, no. 1, pp. 72-80, Feb. 1999.

[11] P. S. Shiakolas, S. R. Van Schenck, D. Piyabongkarn, and I. Frangeskou, "Magnetic levitation hardware-in-the-loop and MATLAB-based experiments for reinforcement of neural network control concepts," *IEEE Trans. Educ.*, vol. 47, no. 1, pp. 33-41, Feb. 2004.

[12] J.-L. Lin, and B.-C. Tho, "Analysis and μ-based controller design for an electromagnetic suspension system," *IEEE Trans. Educ.*, vol. 41, no. 2, pp. 116-129, May 1998.

[13] V. A. Oliveira, E. F. Costa, and J. B. Vargas, "Digital implementation of a magnetic suspension control system for laboratory experiments," *IEEE Trans. Educ.*, vol. 42, no. 4, pp. 315-322, Nov. 1999.

[14] W. G. Hurley, and W. H. Wölfle, "Electromagnetic design of a magnetic suspension system," *IEEE Trans. Educ.*, vol. 40, no. 2, pp. 124-130, May 1997.

[15] W. G. Hurley, and W. H. Wölfle, "PWM control of a magnetic suspension system," *IEEE Trans. Educ.*, vol. 47, no. 2, pp. 165-173, May 2004.

[16] M. Baylie, P. J. Ford, G. P. Mathlin, and C. Palmer, "The jumping ring experiment," *Physics Education*, vol. 44, no. 1, pp. 27-32, Jan. 2009.

[17] Župan, Tomislav; Dadić, Martin; Štih, Željko, "Fully Coupled Dynamic Model of Thomson's Levitating Ring," *IEEE Trans Magn.*, vol. 51 no. 5, pp. 8300209-1-8300209-9, May 2015.

[18] Aluminum 5005-O, HM Wire International, Inc, 2011. Available: http://www.hmwire.com/New%20PDFs/Aluminum_5005_Information.pdf

[19] M. A. Bramson, "Infrared radiation, a handbook for applications", Plenum Press, 1968.

[20] J. T. Conway, "Exact solutions for the magnetic fields of axisymmetric solenoids and current distributions," *IEEE Trans. Mag*, vol. 37, no. 4, pp. 2977-2988, Jul. 2001.

[21] S. Babic and C. Akyel, "Improvement in calculation of the self- and mutual inductance of thin-wall solenoids and disk coils," *IEEE Trans. Mag*, vol. 36, no. 4, pp. 1970-1975, Jul. 2000.

[22] W. S. Janna, "Engineering heat transfer", CRC Press, 2000.

[23] G. Nellis, and S. Klein, "Heat transfer", Cambridge University Press, 2009.

[24] Y. A. Cengel, "Heat transfer: a practical approach", McGraw-Hill, 2002.

[25] W. J. Minkowycz, E. M. Sparrow, J. Y. Murthy, "Handbook of numerical heat transfer", John Wiley & Sons, 2006.

[26] M. Favre-Marinet, S. Tardu, "Convective heat transfer", John Wiley & Sons, 2009.

[27] Electrical steel non oriented fully processed, Cogent Power Ltd, 2002. Available: http://www.sura.se/Sura/hp_products.nsf/